An Interpretation of the Enhancement of the Water Dipole Moment Due to the Presence of Other Water Molecules

Daniel D. Kemp and Mark S. Gordon*

Department of Chemistry, Iowa State University, Ames, Iowa 50011

Received: March 4, 2008

The dipole moment of the gas phase water monomer is 1.85 D. When solvated in bulk water, the dipole moment of an individual water molecule is observed to be enhanced to the much larger value of 2.9 ± 0.6 D. To understand the origin of this dipole moment enhancement, the effective fragment potential (EFP) method is used to solvate an ab initio water molecule to predict the dipole moments for various cluster sizes. The dipole moment as a function of cluster size, $n$$H_2O$, is investigated [for n = 6–20 (even n), 26, 32, 41, and 50]. Localized charge distributions are used in conjunction with localized molecular orbitals to interpret the dipole moment enhancement. These calculations suggest that the enhancement of the dipole moment originates from the decrease of the angle between the dipole vectors of the lone pairs on oxygen as the number of hydrogen bonds to that oxygen increases. Thus, the decreased angle, and the consequent increase in water dipole moment, is most likely to occur in environments with a larger number of hydrogen bonds, such as the center of a cluster of water molecules.

I. Introduction

Water is arguably the most important liquid and solvent, especially for biological and biochemical applications. Despite its broad impact and importance, many properties of water are not fully understood. One important property is the dipole moment of water, which has been the subject of many experimental[1–6] and theoretical[7–52] investigations. Although the dipole moment of the water monomer has been experimentally[1,2,4–6] and computationally[7–9] determined to be 1.85 D, there has been only one experimental report regarding the dipole moment of a water molecule in bulk liquid water: Badyal et al.[3] employed x-ray diffraction experimental techniques to determine that the dipole moment of a solvated water molecule is 2.9 ± 0.6 D.

Many theoretical studies have predicted the dipole moments of water clusters.[9–53] These calculations have employed a variety of methods, including fully ab initio calculations on relatively small clusters[9] (n = 1–6), molecular dynamics simulations on larger clusters using model potentials (n = 216,[13,14] n = 256,[12,15] and n = 512[10]), and a mix of quantum mechanical/molecular mechanical (QM/MM) methods.[17–19] Some studies have focused on the dipole moment of a single water molecule in an ice lattice.[20–23] Each of these studies produces a slightly different result, with most estimating that the dipole moment of a water molecule in the bulk falls in the range of 2.5 –3.5 D.

The methods that use model potentials[10–15,24] that include a polarization term generally predict dipole moments more accurately than those that employ model potentials without polarization. Potentials that include only point charges and electrostatics apparently do not accurately predict the dipole moment enhancement. Dang[11] has developed a polarizable potential and has predicted average dipole moments per water molecule that closely resemble the MP2 study of Gregory[9] et al. for n = 1–6. The NCC model developed by Niesar et al.[10] adds many-body polarizability to a previously developed potential and obtains an average dipole moment of 2.8 D per water molecule in a 512 water molecule cluster.

TABLE 1: Predicted MP2 Dipole Moment for the Water Monomer Using Three Basis Sets[a]

basis set	no. of basis functions	MP2 dipole (D)
DH (d,p)	25	2.17
aug-cc-pVDZ	43	1.88
aug-cc-pVTZ	105	1.85

[a] Computational cost is given in basis functions.

Tu and Laaksonen[18] predicted the dipole moment of one ab initio water molecule solvated by 1–4 water molecules represented by model potentials. The dipole moment of the ab initio water increased to ~2.6 D for n = 4. Molecular dynamics simulations of 256 water molecules yielded an average value of 2.65 D for each water molecule within the cluster.

The present work systematically examines the dipole moment of an ab initio water molecule as a function of the number of additional water molecules that are represented by a sophisticated model potential. In addition, an analysis of the origin of the dipole moment enhancement is presented. The computational methods are presented in section II. Section III presents the Results and Discussion of the calculations. This is followed in section IV by a summary and conclusions.

II. Computational Methods

Dipole moments have been calculated by surrounding a quantum mechanics (QM) water molecule by a cluster of n − 1 effective fragment potential[54,55] (EFP) waters. An EFP is an explicit model potential that is based on QM and implemented in the General Atomic and Molecular Electronic Structure System[56,57] (GAMESS) software suite. The EFP1 method was originally developed to model liquid water interactions. That initial implementation was based on Hartree−Fock (HF), with a goal to reproduce ab initio calculations while requiring significantly less computational effort.[54] This method was later extended to model water at the DFT level of theory.[58] It was demonstrated in the latter work that a combination of EFP1/

10.1021/jp801921f CCC: $40.75
Published on Web 05/13/2008

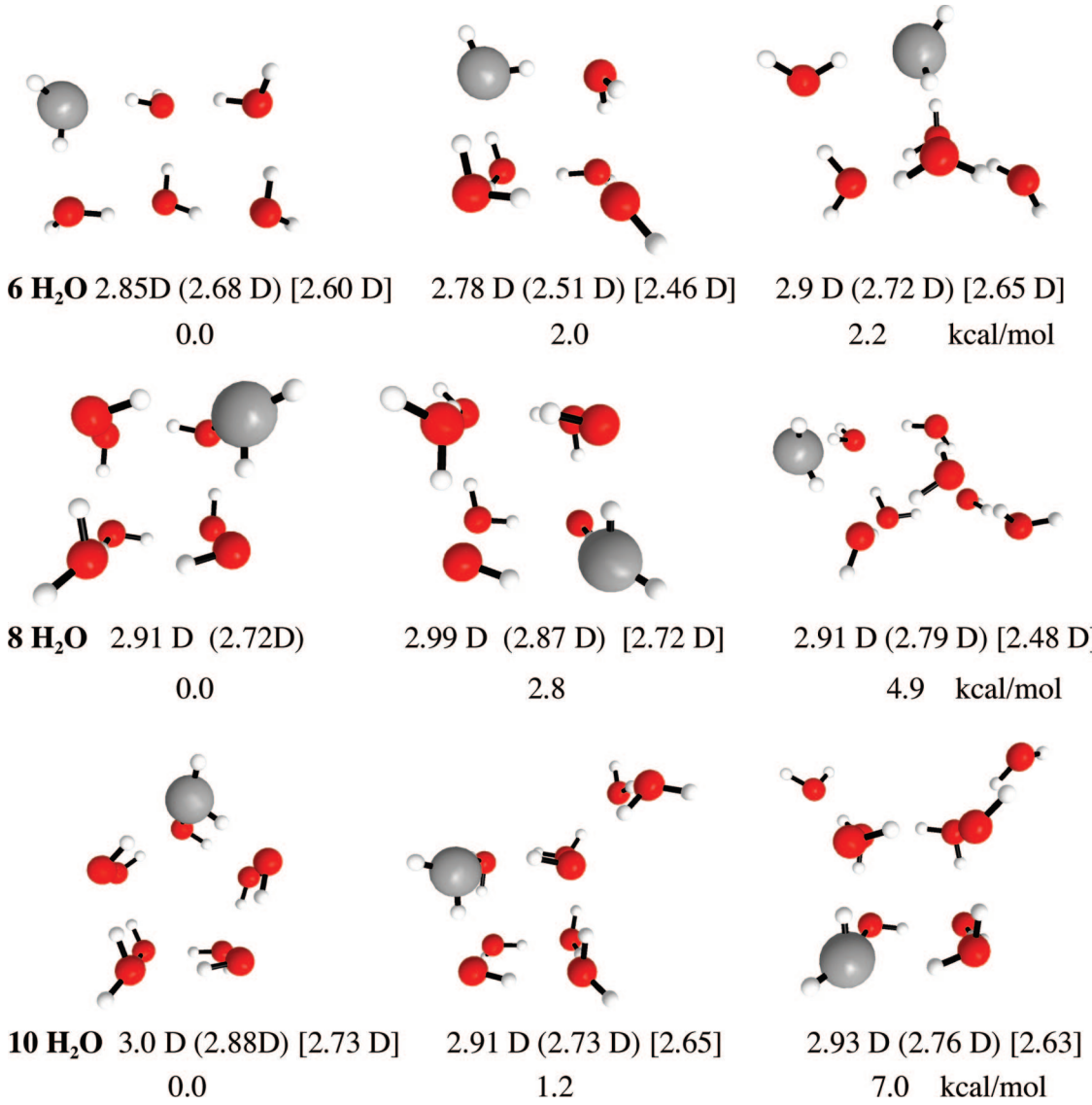

Figure 1. Sample of minima from each cluster size containing six, eight, and 10 water molecules. The DH (d,p) (aug-cc-pVDZ) [aug-cc-pVTZ] dipole (in Debye) of the ab initio water molecule within the cluster is given. The global minimum structure found using aug-cc-pVDZ is given on the left, with two higher energy structures given for each value of n. Relative energy differences (kcal/mol) from the global minimum are given underneath each structure.

DFT waters with an MP2 substrate provides an efficient and accurate representation of a full MP2 calculation. An EFP includes three separate interaction energies: Coulomb, polarization, and exchange repulsion + charge transfer. In each EFP, Coulomb interaction sites are placed at all atom centers and all bond midpoints. Polarizability centers are at the centroids of all LMOs. The DFT-based EFP1 also includes some correlation effects at short range. Because of the success of the EFP1 model[58–61] for water, a more general model called EFP2 has also been developed.[55] EFP2 can be used to generate a model potential for any species, but EFP2 has not yet been fully interfaced with QM. The EFP1/DFT method is used in this paper. The QM water is represented by second order perturbation theory (MP2).[62–65]

For the water monomer, MP2 optimizations were performed using three different basis sets, to assess which basis sets(s) can accurately predict the gas phase water dipole moment: (i) the Dunning−Hay basis set with d and p polarization functions on O and H, respectively [DH(d,p)],[66] (ii) the augmented correlation-consistent double-ζ basis set (aug-cc-pVDZ),[67,68] and (iii) the corresponding triple-ζ basis set (aug-cc-pVTZ).[67,68]

The general approach used here is similar to that employed by Tu and Laaksonen.[18,19] For clusters containing n water molecules, with $n \geq 1$, $n - 1$ waters are represented by EFPs, while the remaining water is described by MP2 with one of the aforementioned basis sets. A Metropolis-based Monte Carlo (MC)[69] method was used in conjunction with simulated annealing[70] (SA) to study clusters that contain up to 50 water molecules. For 6–20 water molecules, the MP2 water molecule is described using the DH(d,p), aug-cc-pVDZ, and aug-cc-pVTZ basis sets. MC sampling on clusters containing 26, 32, 41, and 50 water molecules employed only the DH (d,p) basis. Dipole moments are predicted for the final structures using the larger basis sets. The matrix of energy second derivatives (Hessian) was calculated for each structure to ensure that the structure is a local minimum on the potential energy surface and to provide vibrational zero point energies.

To analyze the calculated dipole moments for various water clusters, the localized charge distribution (LCD)[73,74] method was employed. On the basis of the use of the HF localized molecular orbitals (LMO),[75,76] an LCD is a charge neutral localized system that contains two electrons and two protons. One can therefore

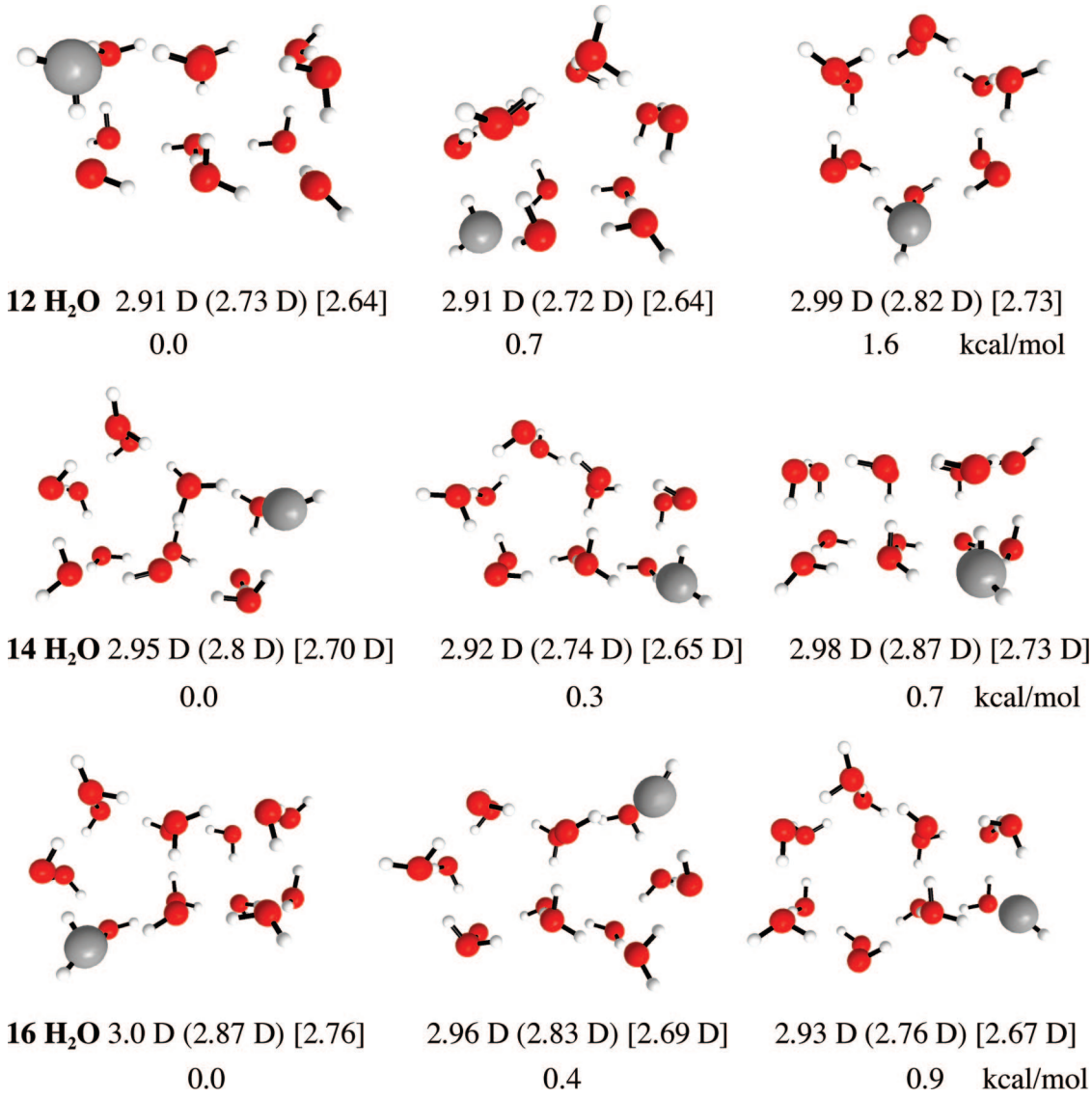

Figure 2. Minimum energy structures for $n = 12$, 14, and 16 H_2O. The same format used for the previous figure is used here.

calculate origin-invariant LCD dipole moments that sum vectorially to the total molecular dipole moment. These LCD dipoles can then be used to analyze the origin of the dipole moment enhancement. For the LMO and LCD calculations, the QM water is represented by HF with the aug-cc-pVTZ basis set, while the remaining waters are represented by EFPs. The LMOs were obtained using the Boys[75] approach first introduced by Edmiston and Ruedenberg.[76] Once the LCDs are determined, individual dipole moments for each LCD can be calculated. Finally, we note that if an entire water cluster were represented by a particular level of electronic structure theory (e.g., MP2) in a supermolecule sense, it would be difficult (although not impossible[77]) to rigorously separate the electron density of each water due to delocalization. Because only one quantum water is present in this work, delocalization effects are not included here.

III. Results and Discussion

A. Water Monomer. As shown in Table 1, MP2/DH(d,p) overestimates the monomer dipole moment by approximately 0.3 D, while MP2/aug-cc-pVDZ and MP2/aug-cc-pVTZ predict monomer dipole moments that are in excellent agreement with the experimental value.[1,2,4–9] Because the aug-cc-pVTZ basis set is significantly more computationally demanding than the other two basis sets, the strategy followed here is to perform geometry optimizations and MC/SA simulations using the two smaller basis sets, followed by single point calculations with the largest basis set.

B. Small Clusters Containing 6–20 Water Molecules. Day et al.[78] have previously performed EFP1/HF Monte Carlo simulations on water clusters $(H_2O)_n$, for even n, ranging in size from 6–20 water molecules. In the present work, the minima from this previous effort were used to initiate MC/SA simulations.

To sample all possible locations for the ab initio water molecule, the MP2/DH(d,p) water molecule was placed at each unique position within the cluster; then, a Monte Carlo simulation was performed. In each case, the lowest energy structure was retained. Once the lowest energy configuration was found for each n, the structure was reoptimized using the DH (d,p) and aug-cc-pVDZ basis sets. Single point energy calculations using the aug-cc-pVTZ basis set were performed at the MP2/aug-cc-pVDZ geometries to predict the dipole moment more accurately.

Example structures and their associated dipole moments for each value of n are given in Figures 1−3. All figures were produced using MacMolPlt.[79] Energies relative to the global

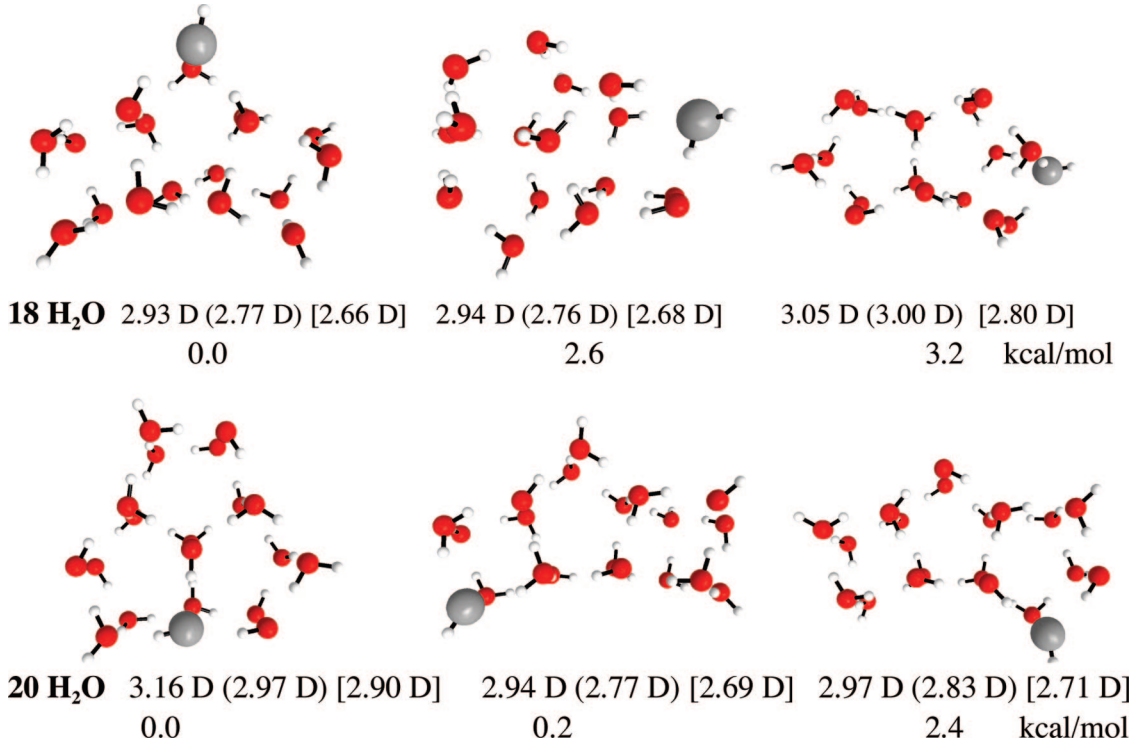

Figure 3. Minima for $n = 18$ and 20. The same format used for the previous two figures is used here.

TABLE 2: Boltzmann Averaged $(H_2O)_n$ MP2 Dipole Moments for $n = 6$–20

	average dipole		
n H_2O	DH (d,p)	aug-cc-pVDZ	aug-cc-pVTZ
6	2.85	2.67	2.54
8	2.91	2.72	2.64
10	3.00	2.87	2.74
12	2.92	2.76	2.70
14	2.93	2.77	2.67
16	2.98	2.82	2.74
18	2.96	2.77	2.67
20	3.11	2.91	2.90

minimum are given in kcal/mol. The MP2/DH(d,p) dipole moment is given followed by the aug-cc-pVDZ dipole moment in parentheses and the aug-cc-pVTZ dipole moment in square brackets.

For each value of n, the Boltzmann averaged dipole moment, shown in Table 2, was determined for $T = 298$ K. As noted above for the water monomer, MP2 with the smaller DH (d,p) basis set consistently predicts dipole moments that are 0.1–0.2 D larger than those predicted by MP2/aug-cc-pVDZ and approximately 0.2–0.3 D larger than MP2/aug-cc-pVTZ. The dipole moment enhancement is apparent even at six waters, for which the predicted MP2/aug-cc-pVTZ dipole moment is already 2.54 D, about 0.7 D larger than that predicted for the water monomer at the same level of theory, and only ~0.4 D less than the experimental value for a water molecule in the bulk environment. This is in good agreement with a previous ab initio study by Gregory et al.[9] in which the MP2 dipole moment of a single water molecule in water hexamer was predicted to be 2.7 D. Although the dipole moment fluctuates a bit as the cluster size grows from 6–20, MP2/aug-cc-pVTZ predicts a Boltzmann averaged dipole moment of 2.90 D for 20 water molecules, close to the experimental value for a water molecule in the bulk.

C. Structures Containing 26, 32, 41, and 50 Water Molecules. Monte Carlo simulations were next performed on larger clusters, to examine convergence of the predicted dipole moment. As the cluster size increases, the extent of required sampling increases, since the number of possible configurations increases. As before, one water molecule was treated with MP2, while all the other waters are represented by EFP1/DFT. Initially, the MP2/DH(d,p) water molecule was placed as close as possible to the center of the water cluster. Of course, no constraints were placed on the Monte Carlo simulations, but experience suggests that dramatic changes in the structure do not occur. Once a sample of structures was found for each cluster size, the results were Boltzmann averaged. Relative energies and sample structures are shown in Figures 4 and 5. The effect of moving the MP2 water molecule to other regions of the cluster is discussed in the next subsection.

The most energetically favorable structures for 26 water molecules are similar to those found for $n = 20$, that is, two planar "sheets" of molecules stacked on top of each other (see structure 26B in Figure 6). For larger clusters (32, 41, and 50), the lowest energy structures are spherical as expected for bulk water, rather than the higher energy stacked planar sheets (structures 32A, 41A, and 50A in Figure 6). The structures that have one water molecule solvated by other water molecules evenly distributed throughout its three dimensional surroundings are considered to be completely solvated. At $n = 32$, the completely solvated structure (32A) is lower in energy than the sheet structure (32B), and this trend is followed for $n = 41$ and 50. The energy difference between the approximately spherical structure (global minimum) and the planar sheet structure increases from 14.3 to 18.1 to 29.1 kcal/mol as n increases from 32 to 41 to 50.

The Boltzmann-averaged dipole moments of an MP2 water molecule placed approximately at the center of 26, 32, 41, and 50 water molecule clusters are given in Table 3. The Boltzmann-averaged dipole moments for the four values of n are similar to each other and slightly fluctuate within the experimental error

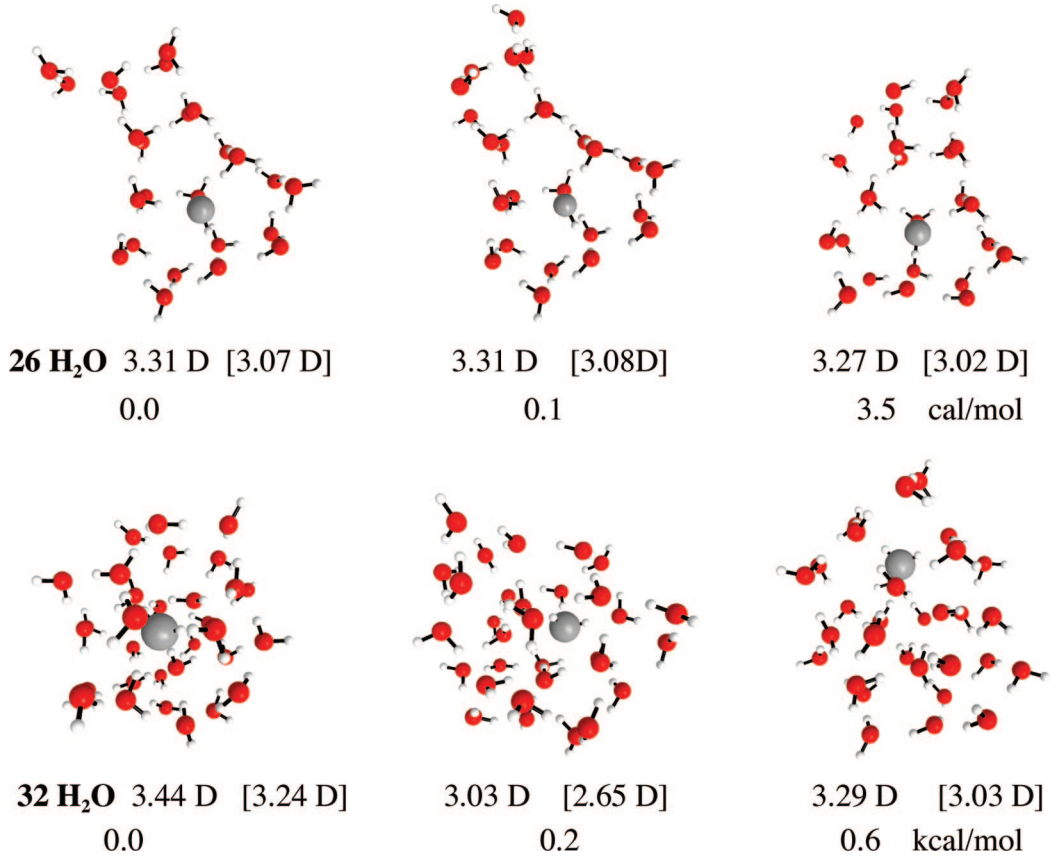

Figure 4. Sample of minima for 26 and 32 water molecules. The left-most structure is the global minimum structure, while the two structures to the right of it are higher energy structures. The oxygen atom of the ab initio water molecule is shaded and larger in size to illustrate where the ab initio water molecule is located within the cluster. Relative energies (in kcal/mol) and DH (d,p) (aug-cc-pVDZ) [aug-cc-pVTZ] dipoles (in Debye) are given underneath each structure.

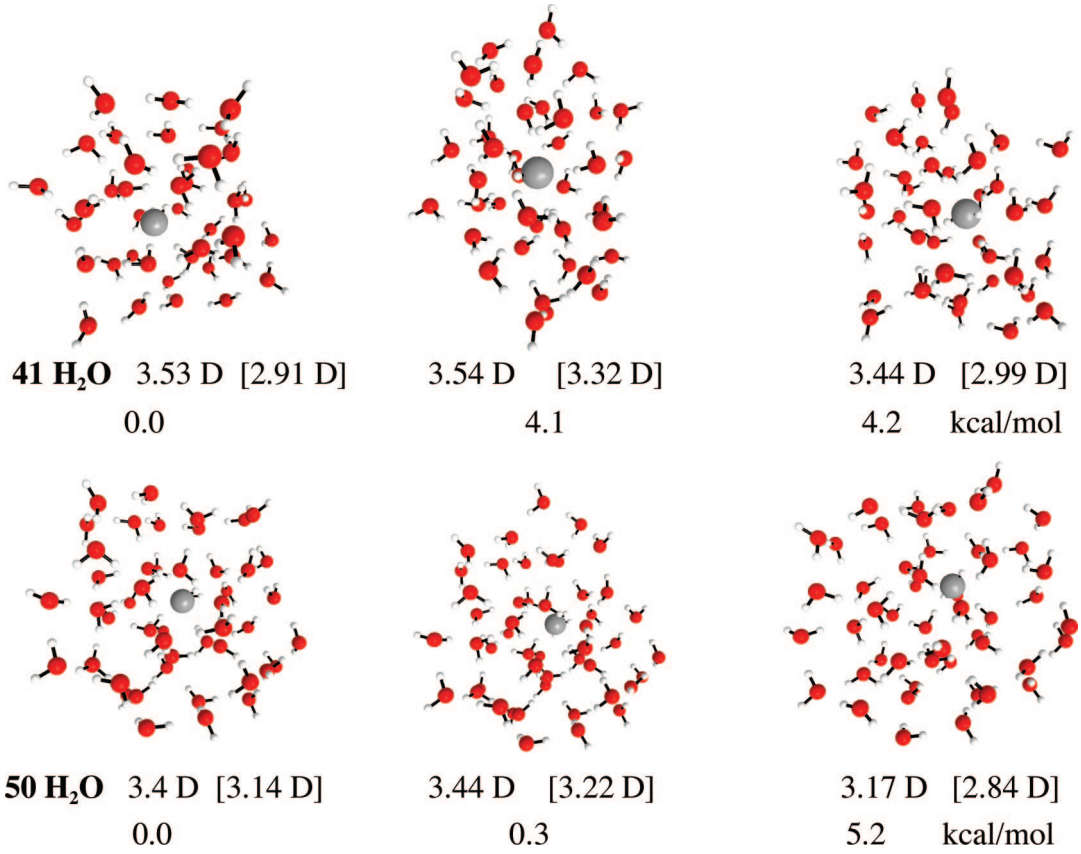

Figure 5. Sample minima for $n = 41$ and 50 H_2O water molecules. The same format and labeling used in Figure 4 is used here.

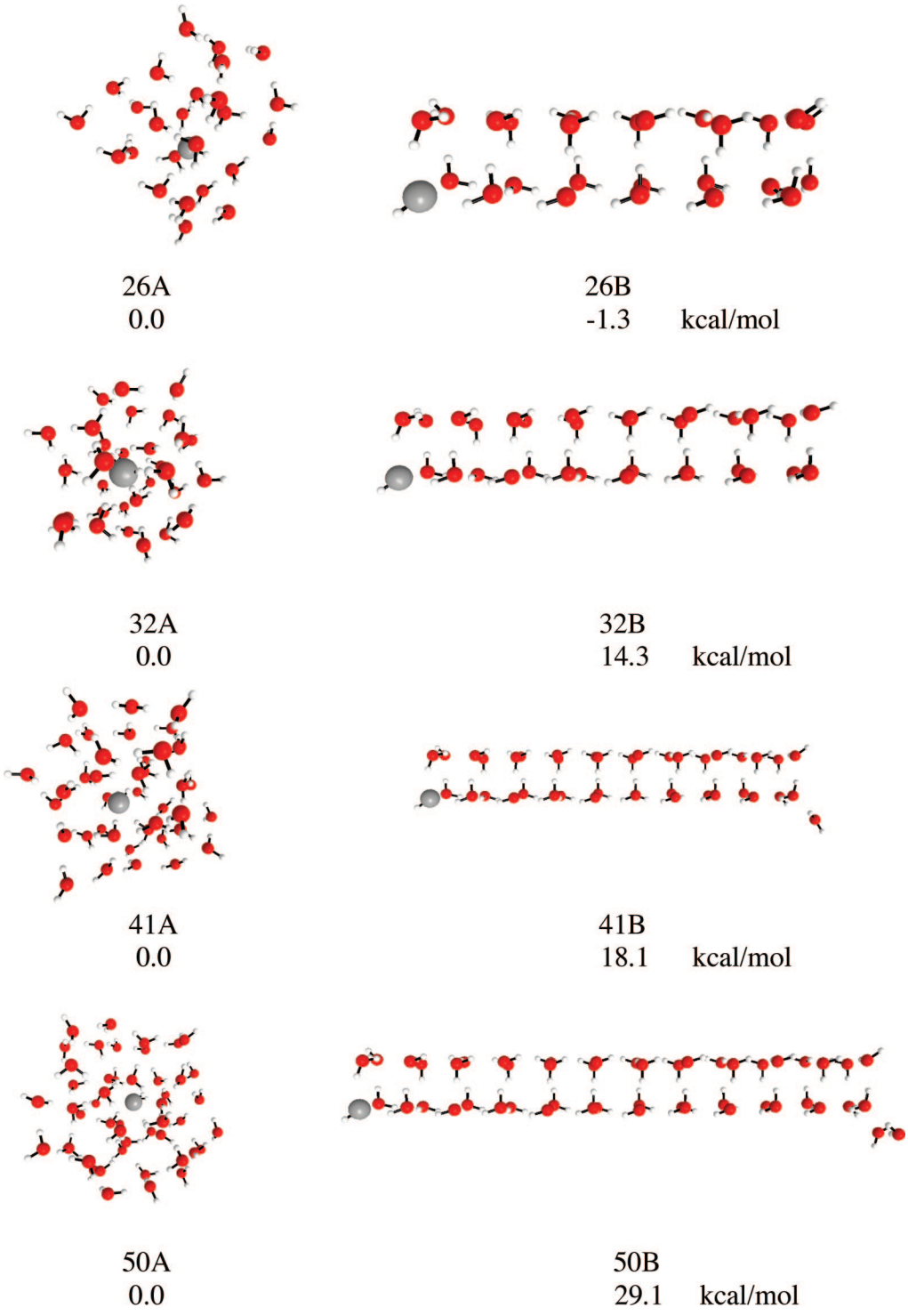

Figure 6. Symmetric structures formed from minima for $n = 26$, 32, 41, and 50. These structures involve parallel planes of four water molecules hydrogen bonded to each other. The four water molecules in each parallel plane hydrogen bond to each other and form the shape of a square. Relative energies are compared to the lowest energy structure, which is comprised of one central water molecule completely solvated and surrounded by the rest of the cluster.

bars given by Badyal et al.[3] (2.9 ± 0.6). As observed for the smaller water clusters, MP2/aug-cc-pVTZ predicts a smaller dipole moment for each cluster size than MP2/DH(d,p), and using the larger basis set yields dipole moments that are closer to the experimental value.

D. Origin of the Dipole Moment. To sample the dipole moment of a single water molecule in various hydrogen-bonding environments throughout water clusters containing $n = 32$ and 41 molecules, an MP2/aug-cc-pVTZ calculation was done at every EFP position in the global minimum structure for each value of n. The location of the MP2 water molecule was moved about the cluster until all positions had been sampled, with the $n - 1$ waters represented by EFPs. The Boltzmann-averaged dipole moments are presented in Table 4. The range presented

TABLE 3: Boltzmann-Averaged Dipole Moments of All Structures Found for 32, 41, and 50 Water Molecules, Using the DH(d,p) and aug-cc-pVTZ Basis Sets and Placing the MP2 Water at the Approximate Center of the Cluster

	average dipole	
cluster size	DH (d,p)	aug-cc-pVTZ
26	3.3	3.1
32	3.3	2.9
41	3.5	3.3
50	3.4	3.2

TABLE 4: Boltzmann-Averaged MP2/aug-cc-pVTZ Dipole Moment (in Debye) for $(H_2O)_{32}$ and $(H_2O)_{41}$[a]

cluster size	average dipole	max value	min value
32	3.1	3.43	2.67
41	3.3	3.37	2.72

[a] The largest dipole moment found in the cluster is given in the column max value, while the smallest value is listed in the min value column.

by the minimum and maximum dipole moments (~0.7 D) is similar to the experimental uncertainty (±0.6 D).[3]

Figure 7 presents a graph that depicts the dependence of the computed dipole moment on the number of hydrogen bonds formed by the MP2 water as it is moved to various positions in the global minimum 32-water cluster. In general, the dipole moment increases as the number of hydrogen bonds increases up to 4 (in which case the water molecule donates two and accepts two hydrogen bonds). This suggests that the dipole moment of a water molecule that is internal in a water cluster will tend to be larger than the dipole moments of a water molecule that resides at or near the surface and forms fewer hydrogen bonds.

Additional analysis shows that hydrogen bonds in which a lone pair on the MP2 water interacts with EFP OH bonds play the most significant role in dipole moment enhancement. This will be referred to in this discussion as a hydrogen bond-accepting arrangement, as opposed to hydrogen bond donating in which the MP2 OH bond is interacting with lone pairs on EFP waters. Figure 8 plots the number of hydrogen bond donors against the predicted dipole moment of each water molecule within the global minimum structure for $n = 32$. It is clear that the dipole moment is enhanced as the number of donating OH hydrogen bonds on the MP2 water increases from 1 to 2. However, the dipole moment is not significantly enhanced when the number of donating hydrogen bonds increases from 0 to 1. For the ranges of dipole moments for which the number of hydrogen bond donors is 1 or 2, the lower half of each range has one hydrogen bond acceptor, while the upper half corresponds to structures in which the MP2 water lone pairs accept two hydrogen bonds. Also, note that in the line in Figure 8 that corresponds to zero MP2 OH hydrogen bond donors, there are two cases with greatly enhanced dipole moments, ~2.85 and 2.95 D. In these cases, the participation of the MP2 water in hydrogen bonding comes from two hydrogen bond acceptors by the two lone pairs on the MP2 water. This indicates that the lone pair orbitals on the MP2 water, which participate in accepting hydrogen bonds, play an important role in the dipole moment enhancement.

LMOs provide an opportunity to understand the origin of the dipole moment enhancement in a chemically intuitive manner. As noted by Pople,[80,81] a bond orbital resembles a quadrupole,[80] with positive centers (nuclei) at each end and a negative charge distribution (electrons) in between. Lone pairs, on the other hand, resemble dipoles, with a positive nucleus at one end and electron density at the other, giving rise to a charge separation. This suggests that the water dipole moment will largely arise from the oxygen lone pairs. This notion can be examined by decomposing the dipole moment of a water molecule into a vector sum of the dipole moments that arise from its bond and lone pair orbitals. Such an analysis is facilitated by using charge neutral LCDs.[73,74] Because LMOs and LCDs are only available at the HF level of theory, dipole moments in this section are reported at this level of theory using the aug-cc-pVTZ basis set. Of course, the HF water dipole moment calculated with a given atomic basis is larger than that predicted by MP2 with the same basis set and, therefore, larger than the experimental value as well. As will be seen below, the HF dipole moment for a water molecule in an EFP cluster is also higher than the corresponding MP2 dipole moment. However, the trends exhibited by the HF dipole moments as the number of EFP water molecules in the cluster increases are the same as those for an MP2 water molecule. So, the following analysis is reasonable. Although this scheme ultimately divides electron density into LMOs, this is not done until the final step.

Of course, any analysis in which an observable (e.g., water dipole moment) is divided into nonobservable components (e.g., OH bond and lone pair dipole moments) is inherently arbitrary and cannot be directly verified experimentally. Nonetheless, such interpretations in terms of commonly used chemical concepts can be very useful. The OH and lone pair LMO orbitals in an isolated (HF) water molecule are modified when this HF water molecule is placed in a cluster of EFP waters, because the orthogonal linear combinations of atomic orbitals in the HF water are modified by the field of the EFP waters via the polarizability term that is iterated to self-consistency within the HF interations.

Now, consider the water monomer and the global minimum for the 32-water cluster, examined in terms of LCDs in Table 5. As noted above, although the HF dipole moments in Table 5 are larger than the corresponding MP2 dipole moments, the trend and the magnitude of the increase in dipole moment are captured by the HF level of theory. As expected based on the previous discussion, the largest contribution to the magnitude of the water monomer dipole moment comes from the two lone pair LMOs (see Figure 9). There is only a small contribution from the two O−H bond orbitals and virtually no contribution from the oxygen inner shell LMO. Because the net dipole moment is the vector sum of the five contributions (two lone pairs, two OH bond pairs, and the inner shell) and because the magnitudes of the lone pair dipole moments are greater than the net molecular dipole moment, it is clear from the top half of Table 5 that the OH dipole moments are oriented in the opposite direction from the lone pair dipole moments and therefore diminish the net dipole moment. Because the magnitudes of the OH bond dipole moments are rather smaller than the lone pair dipole moments, the net water monomer dipole moment is dominated by the lone pair contributions. Nonetheless, the OH bond dipole vectors do play an important quantitative role in determining the overall dipole moment. The same is true for the HF water molecule in a 32-water cluster, discussed in the following paragraphs.

Now, consider the analogous analysis for the "central" (most fully solvated) water in the global minimum for $(H_2O)_{32}$. The ab initio water is again represented by HF/aug-cc-pVTZ, while the remaining water molecules are DFT-based EFPs.

As for the water monomer, the dipole moment for the central water molecule in $(H_2O)_{32}$ is dominated by the contributions

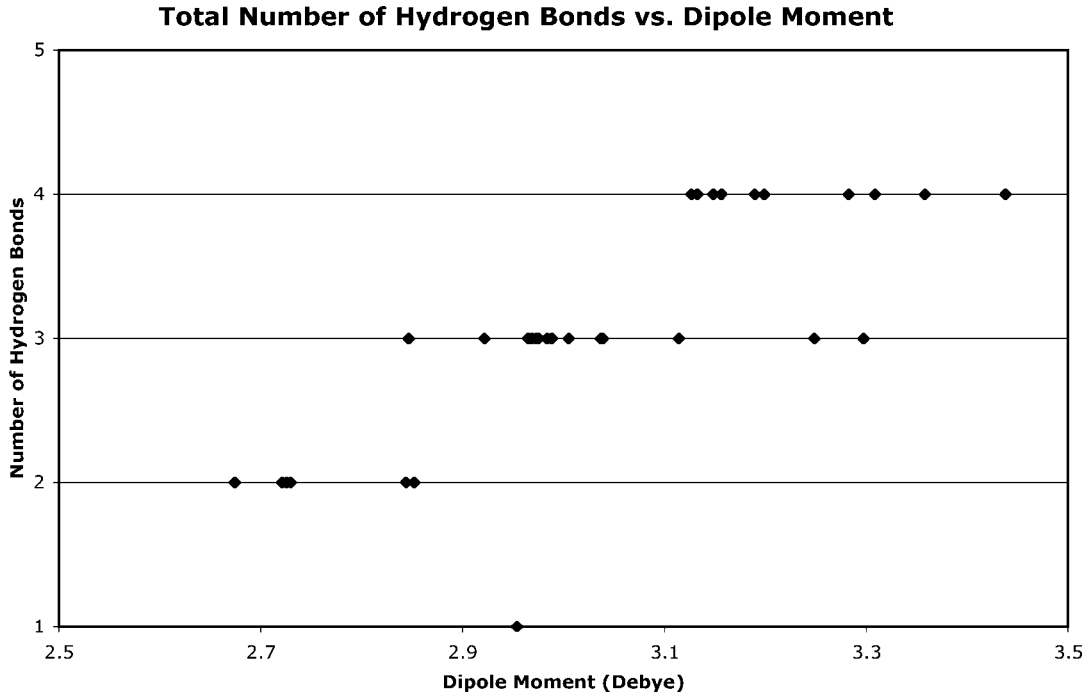

Figure 7. Dipole moment of each water molecule was calculated in the global minimum structure for $n = 32$. The number of hydrogen bonds for each molecule is plotted against the dipole moment for the molecule. In general, increasing the number of hydrogen bonds increases the dipole moment of the molecule.

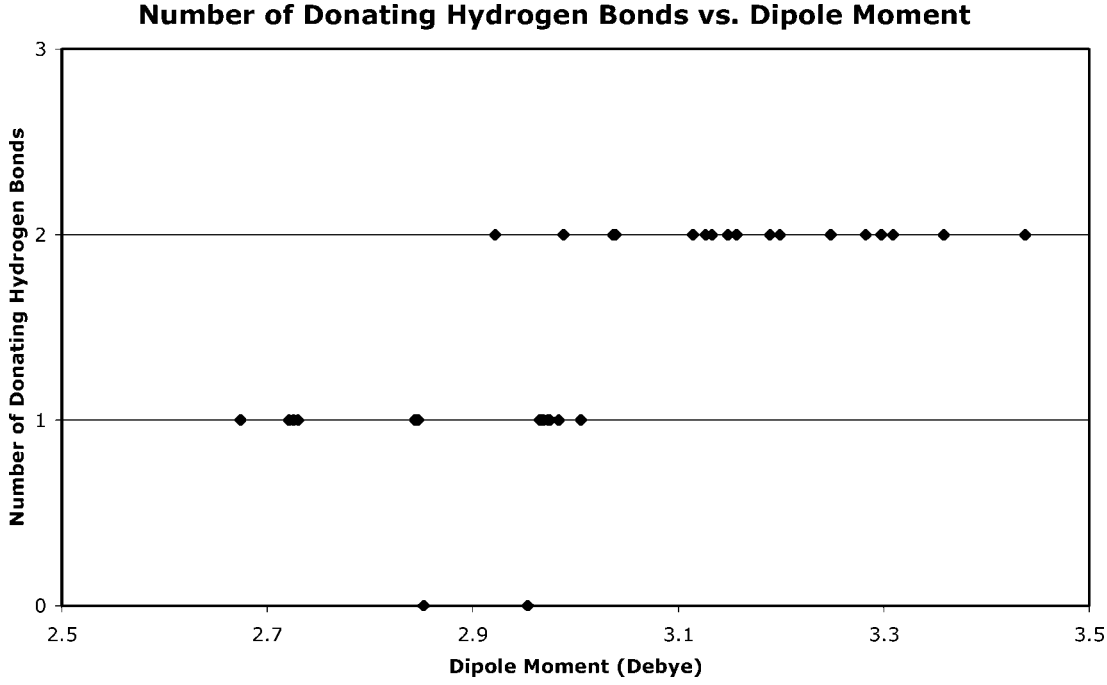

Figure 8. Number of donating hydrogen bonds of each molecule in the $(H_2O)_{32}$ global minimum is plotted against that molecule's predicted dipole moment. Dipole moment enhancement is very large for the two cases where only accepting hydrogen bonds are present.

from the lone pair LMOs (see Table 5). Importantly, the magnitudes of the lone pair dipole moments do not change significantly relative to those of the monomer, nor do those of the bonding LMOs. So, the dipole moment enhancement does not originate from any significant change of the magnitude of the LMO dipole moments. Rather, the dipole moment enhancement is driven by changes in the orientation of the lone pair dipole moments upon solvation. As shown in Table 5, the angle between these lone pair LMO vectors decreases from 124.6° in the monomer to ~117° when solvated by 31 EFPs. This decrease in the angle between the lone pair dipole vectors, expected in a highly hydrogen-bonded environment encountered in liquid or solid water, results in a greater resultant net dipole moment. Once again, the net molecular dipole moment is smaller in magnitude than the lone pair dipole moments because of the opposing OH bond pair dipole moments. Even though the OH dipole moments are much smaller in magnitude, they again have a nontrivial attenuating affect. This behavior is also apparent for $n = 41$ and 50, as may be seen in Table 6. The observed decrease in the angle between the lone pair LMOs arises from

TABLE 5: Dipole Moments for each LMO for the Monomer and for the Center-Most Molecule of the Global Minimum for $n = 32$[a]

orbital no.	orbital type	dipole	lone pair angle
	monomer		
1	core	0	
2	lp	2.88	124.6
3	lp	2.88	
4	bonded	0.39	
5	bonded	0.39	
		1.99	
	32 GM		
1	core	0	
2	lp	3.07	116.8
3	lp	3.12	
4	bonded	0.16	
5	bonded	0.08	
		3.3	

[a] The first column numbers each LMO. The second column describes the type of LMO. The next column gives (in Debye) dipole vector magnitudes and the molecular dipole moment. The angles between lone pair dipole vectors are given in the last column.

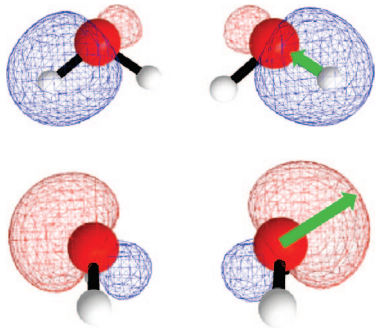

Figure 9. Illustrations of LMOs and the dipole moments along each orbital. The two green arrows illustrate a dipole moment vector lying along a oxygen−hydrogen bond orbital and along an oxygen lone pair.

TABLE 6: Localized Orbital Dipoles and Angles between the Localized Dipole Vectors for the Global Minimum Structures for $n = 41$ and 50

orbital no.	orbital type	dipole	lone pair angle
	41 GM		
1	core	0	
2	lp	3.08	117.5
3	lp	3.08	
4	bonded	0.16	
5	bonded	0.12	
		3.3	
	50 GM		
1	core	0	
2	lp	3.05	117.5
3	lp	3.08	
4	bonded	0.15	
5	bonded	0.09	
		3.21	

the formation of the hydrogen bonds to these lone pairs, thereby increasing the bonding character of these orbitals.

IV. Conclusions

The dipole moment of water has been examined starting with the monomer and systematically adding EFP water molecules to the cluster. Even a small number of water molecules serves to significantly increase the dipole moment of the quantum water. Clusters as small as 6–20 water molecules reproduce the experimentally observed dipole moment enhancement, and clusters with 26, 32, 41, and 50 water molecules agree with each other and with the experimentally observed dipole moment in bulk water.

Numerous papers cite polarization[18,23,24,32,36,41,42,44,51] due to the hydrogen bonding in the liquid environment as a reason for the dipole moment enhancement. Larger induced dipoles have been proposed to be the result of larger polarization effects due to hydrogen bonding. The present work has employed a LCD analysis to illustrate that the dipole moment of both an isolated water molecule and a water molecule in the presence of a cluster of EFP waters is derived primarily from the water lone pairs, attenuated by opposing OH dipole vectors. It then follows that the enhancement of the dipole moment of a water molecule in the presence of other water molecules arises primarily from decreases in the angles between the lone pair dipole vectors. This angle decrease arises in turn from the increased participation of these lone pairs in hydrogen bonds when a water molecule is surrounded by other waters. This analysis is based on an interpretation of an observable (the water dipole moment) in terms of nonobservable components (OH bond and lone pair dipole moments). Even though such approaches are difficult to verify experimentally, such interpretations in terms of commonly used chemical concepts can be very useful.

Acknowledgment. Funding for this study was provided by the Ames Laboratory and the Department of Energy. We thank Dr. Paul Day and Dr. Heather Netzloff for providing initial cluster geometries and Professor Hans Stauffer for interesting and helpful discussions.

References and Notes

(1) Shostak, S. L.; Ebenstein, W. L.; Muenter, J. S. *J. Chem. Phys.* **1991**, *94*, 5875.
(2) Shostak, S. L.; Ebenstein, W. L.; Muenter, J. S. *J. Chem. Phys.* **1991**, *94*, 5883.
(3) Badyal, Y. S.; Saboungi, M.-L.; Price, D. L.; Shastri, S. D.; Haeffner, D. R.; Soper, A. K. *J. Chem. Phys.* **2000**, *112*, 9206.
(4) Dyke, T. R.; Mack, K. M.; Muenter, J. S. *J. Chem. Phys.* **1977**, *66*, 498.
(5) Clough, S. A.; Beers, Y.; Klein, G. P.; Rotham, L. S. *J. Chem. Phys.* **1973**, *59*, 2254.
(6) Dyke, T. R.; Muenter, J. S. *J. Chem. Phys.* **1973**, *59*, 3125.
(7) Xantheas, S. S.; Dunning, T. H., Jr *J. Chem. Phys.* **1993**, *99*, 8774.
(8) Swanton, D. J.; Bacskay, G. B.; Hush, N. S. *J. Chem. Phys.* **1986**, *84*, 5715.
(9) Gregory, J. K.; Clary, D. C.; Liu, K.; Brown, M. G.; Saykally, R. J. *Science* **1997**, *275*, 814.
(10) Niesar, U.; Corongiu, G.; Clementi, E.; Kneller, G. R.; Bhattacharya, D. K. *J. Phys. Chem.* **1990**, *94*, 7949.
(11) Dang, L. X. *J. Phys. Chem. B* **1998**, *102*, 620.
(12) Rick, S. W.; Stuart, S. J.; Berne, B. J. *J. Chem. Phys.* **1994**, *101*, 614.
(13) Stillinger, F. H.; Rahman, A. *J. Chem. Phys.* **1974**, *60*, 1545.
(14) Ahlstrom, P.; Wallqvist, A.; Engstrom, S.; Jonsson, B. *Mol. Phys.* **1989**, *68*, 563.
(15) Caillol, J. M.; Levesque, D.; Weis, J. J.; Kusalik, P. G.; Patey, G. N. *Mol. Phys.* **1985**, *55*, 65.
(16) Fois, E.S.; Sprik, M.; Parrinello, M. *Chem. Phys. Lett.* **1994**, *223*, 411–415.
(17) Wei, B.; Salahub, D. R. *Chem. Phys. Lett.* **1994**, *224*, 291.
(18) Tu, Y.; Laaksonen, A. *Chem. Phys. Lett.* **2000**, *329*, 283.
(19) Tu, Y.; Laaksonen, A. *J. Chem. Phys.* **1999**, *111*, 7519.
(20) Gatti, C.; Silvi, B.; Colonna, F. *Chem. Phys. Lett.* **1995**, *247*, 135–141.
(21) Heggie, M. I.; Latham, C. D.; Maynard, S. C. P.; Jones, R. *Chem. Phys. Lett.* **1996**, *249*, 485–490.
(22) Reis, H.; Raptis, S. G.; Papadopoulos, M. G. *Chem. Phys.* **2001**, *263*, 302–316.
(23) Coulson, C. A.; Eisenberg, D. *Proc. R. Soc. London* **1966**, *291*, 445.

(24) Chialvo, A. A.; Cummings, P. T. *J. Chem. Phys.* **1996**, *105*, 8274.
(25) Bursulaya, B. D.; Jeon, J.; Zichi, D. A.; Kim, H. J. *J. Chem. Phys.* **1998**, *108*, 3286.
(26) Delle Site, L.; Alavai, A.; Lynden-Bell, R. M. *Mol. Phys.* **1999**, *96*, 1683.
(27) Rick, S. W. *J. Chem. Phys.* **2001**, *114*, 2276.
(28) Svishchev, I. M.; Kusalik, P. G.; Wang, J.; Boyd, R. J. *J. Chem. Phys.* **1996**, *105*, 4742.
(29) Batista, E. R.; Xantheas, S. S.; Jonsson, H. *J. Chem. Phys.* **2000**, *112*, 3285.
(30) Whalley, E. *Chem. Phys. Lett.* **1978**, *53*, 449.
(31) Liu, K.; Brown, M. G.; Saykally, R. J. *J. Chem. Phys. A* **1997**, *101*, 8995.
(32) Dang, L. X.; Chang, T.-M. *J. Chem. Phys.* **1997**, *106*, 8149.
(33) Sprik, M.; Klein, M. L. *J. Chem. Phys.* **1988**, *89*, 7556.
(34) Whalley, E. *Chem. Phys. Lett.* **1978**, *53*, 449.
(35) Xantheas, S. S. *J. Chem. Phys.* **1995**, *102*, 4505.
(36) Batista, E. R.; Xantheas, S. S.; Jonsson, H. *J. Chem. Phys.* **1998**, *109*, 4546.
(37) Bernardo, D. N.; Ding, Y.; Krogh-Jespersen, K.; Levy, R. M. *J. Phys. Chem.* **1994**, *98*, 4180.
(38) Xantheas, S. S.; Dunning, T. H., Jr *J. Chem. Phys.* **1993**, *98*, 8037.
(39) Kozack, R. E.; Jordan, P. C. *J. Chem. Phys.* **1992**, *92*, 3120.
(40) Zhu, S.-B.; Sing, S.; Robinson, G. W. *J. Chem. Phys.* **1991**, *95*, 2791.
(41) Cieplak, P.; Kollman, P.; Lybrand, T. *J. Chem. Phys.* **1990**, *92*, 6755.
(42) Silvestrelli, P. L.; Parrinello, M. *Phys. Rev. Lett.* **1999**, *82*, 3308.
(43) Sprik, M. *J. Chem. Phys.* **1991**, *95*, 6762.
(44) Gubskaya, A. V.; Kusalik, P. G. *J. Chem. Phys.* **2002**, *117*, 5290.
(45) Brodholt, J.; Sampoli, M.; Vallauri, R. *Mol. Phys.* **1995**, *85*, 81.
(46) Rocha, W. R.; Coutinho, K.; de Almeida, W. B.; Canuto, S. *Chem. Phys. Lett.* **2001**, *335*, 127.
(47) Carnie, S. L.; Patey, G. N. *Mol. Phys.* **1982**, *47*, 1129.
(48) Field, M. J. *Mol. Phys.* **1997**, *91*, 835.
(49) Caldwell, J.; Dang, L. X.; Kollman, P. A. *J. Am. Chem. Soc.* **1990**, *112*, 9144.
(50) Batista, E. R.; Xantheas, S. S.; Jonsson, H. *J. Chem. Phys.* **1999**, *111*, 6011.
(51) Barnes, P.; Finney, J. L.; Nicholas, J. D.; Quinn, J. E. *Nature* **1979**, *282*, 459.
(52) Kusalik, P. G.; Svishchev, I. M. *Science* **1994**, *265*, 1219.
(53) (a) McGrath, M. J.; Siepmann, J. I.; Kuo, I.-F. W.; Mundy, C. J. **2007**, *10*, 1411. (b) Laasonen, K.; Sprik, M.; Parrinello, M.; Car, R. *J. Chem. Phys.* **1993**, *99*, 9080.
(54) Day, P. N.; Jensen, J. H.; Gordon, M. S.; Webb, S. P.; Stevens, W. J.; Krauss, M.; Garmer, D.; Basch, H.; Cohen, D. *J. Chem. Phys.* **1996**, *105*, 1968.
(55) Gordon, M. S.; Freitag, M. A.; Bandyopadhyay, P.; Jensen, J. H.; Kairys, V.; Stevens, W. J. *J. Phys. Chem. A* **2001**, *105*, 293.
(56) Schmidt, M. W.; Baldridge, K. K.; Boatz, J. A.; Jensen, J. H.; Koseki, S.; Matsunaga, N.; Gordon, M. S.; Ngugen, K. A.; Su, S.; Windus, T. L.; Elbert, S. T.; Montgomery, J.; Dupuis, M. *J. Comput. Chem.* **1993**, *14*, 1347.
(57) Gordon, M. S.; Schmidt, M. W. Advances in electronic structure theory: GAMESS a decade later. In *Theory and Applications of Computational Chemistry*; Dykstra, C. E., Frenking, G., Kim, K. S., Scuseria, G. E., Eds.; Elsevier: Amsterdam, 2005; Chapter 41.
(58) Adamovic, I.; Freitag, M. A.; Gordon, M. S. *J. Chem. Phys.* **2003**, *118*, 6725.
(59) Webb, S. P.; Gordon, M. S. *J. Phys. Chem. A* **1999**, *103*, 1265.
(60) Adamovic, I.; Gordon, M. S. *J. Phys. Chem. A* **2005**, *109*, 1629.
(61) Day, P. N.; Pachter, R.; Gordon, M. S.; Merrill, G. N. *J. Chem. Phys.* **2000**, *112*, 2063.
(62) Pople, J. A.; Binkley, J. S.; Seeger, R. *Int. J. Quantum Chem. Symp.* **1976**, *10*, 1.
(63) Frisch, M. J.; Head-Gordon, M.; Pople, J. A. *Chem. Phys. Lett.* **1990**, *166*, 275.
(64) Fletcher, G. D.; Schmidt, M. W.; Gordon, M. S. *Adv. Chem. Phys.* **1999**, *110*, 267.
(65) Aikens, C. M.; Webb, S. P.; Bell, R. L.; Fletcher, G. D.; Schmidt, M. W.; Gordon, M. S. *Theor. Chem. Acc.* **2003**, *110*, 233.
(66) Dunning, T. H.; Hay, P. J. In *Methods of Electronic Structure Theory*; Shaefer, H. F., III, Ed.; Plenum Press: New York, 1977; pp 1–27.
(67) Dunning, T. H., Jr *J. Chem. Phys.* **1989**, *90*, 1007.
(68) Kendall, R. A.; Dunning, T. H., Jr.; Harrison, R. J. *J. Chem. Phys.* **1992**, *96*, 6769.
(69) Metropolis, N.; Rosenbluth, A.; Tellor, A. *J. Chem. Phys.* **1953**, *21*, 1089.
(70) Kirkpatrick, S.; Gelatt, C. D.; Vecchi, M. P. *Science* **1983**, *220*, 671.
(71) Parr, R. G.; Yang, W. *Density Functional Theory of Atoms and Molecules*; Oxford Scientific: Oxford, 1981.
(72) Koch, W.; Holthausen, M. C. *A Chemist's Guide to Density Functional Theory*; Wiley-VCH: Weinheim, 2001.
(73) Jensen, J. H.; Gordon, M. S. *J. Phys. Chem.* **1995**, *99*, 8091.
(74) Remer, L. C.; Jensen, J. H. *J. Phys. Chem.* **2000**, *104*, 9266.
(75) Boys, S. F. In *Quantum Science of Atoms, Molecules, and Solids*; Lowdin, P. O., Ed.; Academic Press: New York, 1966; pp 253–262.
(76) Edmiston, C.; Ruedenberg, K. *Rev. Mod. Phys.* **1963**, *35*, 457.
(77) Bader, R. F. W.; Nguyen-Dang, T. T. *Adv. Quantum Chem.* **1981**, *14*, 63–124.
(78) Day, P. N.; Pachter, R.; Gordon, M. S.; Merrill, G. N. *J. Chem. Phys.* **2000**, *112*, 2063.
(79) Bode, B. M.; Gordon, M. S. *J. Mol. Graphics Modell.* **1998**, *16*, 133–138.
(80) Pople, J. A. *Proc. R. Soc. London* **1951**, *A205*, 155.
(81) Pople, J. A. *Proc. R. Soc. London* **1950**, *A202*, 323.

JP801921F